Changes in Precipitation Extremes in the Hawaiian Islands in a Warming Climate

PAO-SHIN CHU, YING RUAN CHEN, AND THOMAS A. SCHROEDER

Department of Meteorology, School of Ocean and Earth Science and Technology, University of Hawaii at Manoa, Honolulu, Hawaii

(Manuscript received 23 October 2009, in final form 29 April 2010)

ABSTRACT

For the first time, trends of five climate change indices related to extreme precipitation events in the Hawaiian Islands are investigated using daily observational records from the 1950s to 2007. Four indices [simple daily intensity index (SDII), total number of day with precipitation ≥25.4 mm (R25), annual maximum consecutive 5-day precipitation amount (R5d), and the fraction of annual total precipitation from events exceeding the 1961–90 95th percentile (R95p)] describe the intensity (SDII), frequency (R25), and magnitude (R5d and R95p) of precipitation extremes, and the fifth index [consecutive dry days (CDD)] describes drought conditions. The annual probability density functions (PDFs) of precipitation indices for two epochs (i.e., 1950–79 and 1980–2007) are analyzed. Since the 1980s, there has been a change in the types of precipitation intensity, resulting in more frequent light precipitation and less frequent moderate and heavy precipitation intensity. The other three precipitation-related indices (R25, R5d, and R95p) demonstrate a shift toward the left of the distribution over time, suggesting shorter annual number of days with intense precipitation and smaller consecutive 5-day precipitation amounts and smaller fraction of annual precipitation due to events exceeding the 1961–90 95th percentile in the recent epoch relative to the first epoch. The changes of PDF distribution for SDII, R25, R5d, and CDD are significant at the 5% level according to a two-sample Kolmogorov–Smirnov test.

A nonparametric trend analysis is then performed for four periods, with different starting years (e.g., the 1950s, the 1960s) but the same ending year (2007). Long-term downward trends are evident for four precipitation-related indices, and long-term upward trends are observed for CDD. Geographically, Kauai and Oahu are dominated by long-term decreasing trends for four precipitation-related indices, while increasing trends play the major role over the island of Hawaii. The upward trends of drought conditions in the long run are predominant on all the major Hawaiian Islands.

To investigate whether the trends are stable throughout the time, the derivatives of trends for each of the 30-yr running series are calculated (e.g., 1950–79, 1951–80, ... , 1978–2007) for four precipitation-related indices at each station. For Kauai and Oahu, positive derivatives prevail for all indices in the presence of long-term negative trends, suggestive of a phase change in precipitation extremes and such extremes showing an upswing recently. For the island of Hawaii, there is also an indication of phase reversal over the last 60 yr, with negative derivatives occurring in the presence of the background positive trends.

A positive relationship is found between the precipitation indices and the Southern Oscillation index (SOI), implying more precipitation extremes during La Niña years and vice versa for El Niño years. Spatial patterns of standardized anomalies of indices are presented for the La Niña/−PDO minus El Niño/+PDO composites.

1. Introduction

It is well known that earth is undergoing an unprecedented warming process since the Industrial Revolution. According to the Fourth Assessment Report (AR4) of the Intergovernmental Panel on Climate Change (IPCC; Solomon et al. 2007), the rate of the global average surface temperature increased by 0.074°C ± 0.018°C decade^{-1} over the past 100 yr (1906–2005). Since 1981, the rate of warming is faster, with a value of approximately 0.177°C ± 0.052°C decade^{-1}. Consistent with the global warming trend, Hawaii temperature experienced an upward trend as well (Giambelluca et al. 2008): 0.043°C decade^{-1} for the period of 1919–2006 and 0.163°C decade^{-1} for the past 30 yr.

Corresponding author address: Pao-Shin Chu, Department of Meteorology, School of Ocean and Earth Science and Technology, University of Hawaii at Manoa, Honolulu, HI 96822.
E-mail: chu@hawaii.edu

DOI: 10.1175/2010JCLI3484.1

Under this warming background, it is expected that extreme events in temperature and precipitation (PRCP), such as heat waves and heavy rainfall, are changing over time. The occurrence of extreme events is usually a concern for society because of their potential damage to humans, property, public infrastructure, agriculture, and others. To better monitor and understand the variations of extreme events, the Climate Variability and Predictability (CLIVAR) program, an international research entity under the World Meteorological Organization/World Climate Research Programme (WCRP), has developed a suite of climate change indices. These indices are also widely accepted tools to estimate simulation results from climate models, as exemplified by the AR4 of the IPCC.

Global-scale studies of changes in climate extremes using actual observations appeared early in the first decade of the twenty-first century. Using global daily station data, Frich et al. (2002) found an increase in the number of warm summer nights, a decrease in the annual number of frost days, and a significant increase in the total wet day rainfall. Alexander et al. (2006) also noticed a general increase in the precipitation indices globally. Also, midlatitude station data display a tendency toward wetter conditions for 1979–2003 compared with 1901–50. In the regional analyses, Klein Tank and Können (2003), using daily data from 1946 to 1999, detected Europe-wide wet extremes increasing. Moberg and Jones (2005) noted significant increasing precipitation trends over the twentieth century in winter for both average precipitation intensity and moderately strong events in central and western Europe. Griffiths and Bradley (2007) suggested there are positive trends in the northeastern U.S. precipitation extreme indices. Other studies have been conducted to investigate changes in temperature and precipitation extremes during the twentieth century in China (Zhai et al. 1999), India (Roy and Balling 2004), and in the Caribbean region (Peterson et al. 2002).

Transient experiments have been carried out to understand extreme climate changes caused by both historical forcing for the twentieth century and scenario forcings for the twenty-first century (e.g., Kharin and Zwiers 2000). Globally, larger changes in extreme precipitation relative to changes in mean precipitation are shown. Using a multimodel analysis, Tebaldi et al. (2006) analyzed global average time series of extremes and found that the simulated increases in precipitation intensity during the twentieth century continue through the twenty-first century. On the other hand, in all scenarios, the dry periods between precipitation events display a somewhat weaker and less consistent trend of increasing.

In this study, for the first time, five of the core climate change indices suggested by CLIVAR are applied to Hawaii daily precipitation data to investigate the possible changes of extremes. Subsequently, their relationships with El Niño–Southern Oscillation (ENSO) and the Pacific decadal oscillation (PDO) are examined. The structure of this paper is as follows. Section 2 describes the precipitation data analyzed and the definition of five core climate change indices, followed by a description of the methodology in section 3. Section 4 discusses the temporal and spatial characteristics of climate change indices in Hawaii. The relationship between indices and ENSO and the PDO is provided in section 5 and conclusions are found in section 6.

2. Data and climate change indices

a. Data

Daily precipitation data of cooperative (COOP) stations, which are available from the Web site of the National Oceanic and Atmospheric Administration (NOAA)/National Climatic Data Center (NCDC), are used. The orientation map of the Hawaiian Islands is shown in Fig. 1. To keep the wet season data intact, the water year is defined from July to June of the next year. Similarly, the winter season runs from November through April. The starting year of a water year or winter season is chosen to represent that year or season. For example, 1950 means from July 1950 to June 1951, while the 1950 winter season means from November 1950 to April 1951. The COOP dataset is from July 1950 to June 2008. To maintain data quality, some criteria are applied to the climate change indices; this is in reference to those adopted in the Western Regional Climate Center (WRCC) and other researchers (e.g., Griffiths and Bradley 2007). These criteria include the following:

1) A month is considered as having complete data if there are $\leq$5 missing days.
2) A year is considered complete if all months are complete according to item 1.
3) A station series is considered complete if it has equal to or more than 65% complete years according to item 2 in different periods. In our case, a station series is considered complete if it has equal to or more than 38 years' complete record in the period from 1950 to 2007, or if it has equal to or more than 32 years' complete record in the period from 1960 to 2007, and so on.

Applying these criteria to the COOP datasets, the numbers of stations available for the analysis for various periods are listed in Table 1. Clearly, there are more stations as time approaches recent years.

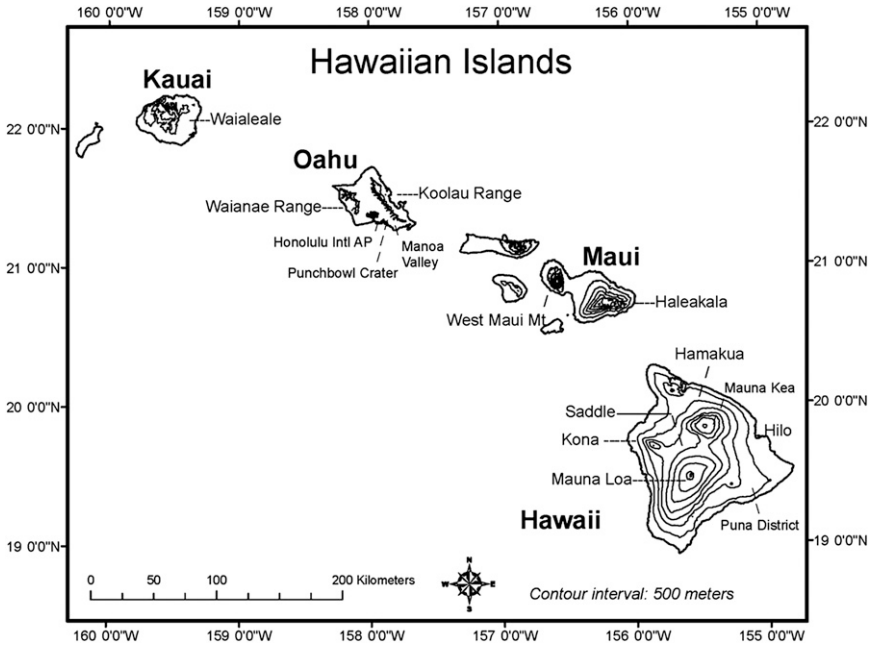

FIG. 1. Orientation map of the Hawaiian Islands; contour interval for elevation is 500 m.

b. Climate change indices

A total of 5 of the 27 indices defined by the joint World Meteorological Organization Commission for Climatology (CC1)/WCRP project on CLIVAR Expert Team on Climate Change Detection, Monitoring and Indices (ETCCEMI) have been included in this research. This set of indices assesses not only different aspects of precipitation, including its intensity, frequency, and magnitude, but also dryness conditions. The definitions of the indices are given in Table 2 (more details about these indices are available online at http://cccma.seos.uvic.ca/ETCCDMI/list_27_indices.shtml).

In Table 2, the simple daily intensity index (SDII) estimates the average wet day precipitation intensity. A wet day is defined as a day with daily precipitation $\geq$1 mm. The unit of SDII is millimeters per day. For simplicity, it is also called precipitation intensity. The R25, a threshold index that provides frequency of intense precipitation, is the annual total number of day with precipitation $\geq$25.4 mm (1 in.). Accordingly, the unit of R25 is days. We recognize that daily precipitation amounts of 25.4 mm may not be ''intense'' for wet regions in Hawaii, but it is indeed a pronounced amount in dry regions such as Waikiki, Oahu, where the mean annual precipitation is 600 mm. R5d is the annual maximum consecutive 5-day precipitation amount, with units in millimeters. Similar to R5d, another index related to the magnitude of intense rainfall is the percentile-based R95p, which by definition is the fraction of annual total precipitation from events exceeding the 1961–90 95th percentile. The unit of R95p is percentage. These four indices are related to the wetness conditions. The fifth index, consecutive dry days (CDD), is the annual maximum number of consecutive dry days; it defines the duration of excessive dryness, and the units are days. Note that small wetness indices do not necessarily imply large CDD values. For example, if CDD is large, but precipitation events are intense and concentrated in several days, then SDII would be large too.

3. Methodology for trend detection

a. A two-sample K–S test

Because the numbers of stations change with different periods, a two-sample Kolmogorov–Smirnov test is used to test whether the difference in station numbers leads to a change of indices' characteristics. A two-sample *K–S* test compares two batches of data under the null hypothesis that they were drawn from the same but unspecified distribution. Using the statistic

$$D_S = \max_x |F_{m_1}(x_1) - F_{m_2}(x_2)| \quad (1)$$

TABLE 1. Number of COOP stations in Hawaii during different periods.

COOP station numbers			
1950s–2007	1960s–2007	1970s–2007	1980s–2007
37	41	50	65

TABLE 2. Definition of the five indices for PRCP extremes.

Index	Definition	Unit
SDII	Simple PRCP intensity index Let RR_{wj} be the daily PRCP amount on wet days, w (RR $\geq$ 1 mm) in period j. If W represents number of wet days in j, then $\mathrm{SDII}_j = \dfrac{\sum_{w=1}^{W} RR_{wj}}{W}$.	mm day^{-1}
R25	Annual count of days when PRCP $\geq$ 25.4 mm Let RR_{ij} be the daily PRCP amount on day i in period j. Count the number of days when $RR_{ij} \geq 25.4$ mm.	days
R5d	Annual maximum consecutive 5-day PRCP Let RR_{kj} be the PRCP amount for the 5-day interval ending k, period j. Then the maximum 5-day values for period j are $\mathrm{R5d}_j = \max(RR_{kj})$.	mm
R95p	Fraction of annual total PRCP due to events exceeding the 1961–90 95th percentile Let RR_{wj} be the daily PRCP amount on a wet day w (RR $\geq$ 1.0 mm) in period j, and let $RR_{wn}95$ be the 95th percentile of PRCP on wet days in the 1961–90 period. If W represents the number of wet days in the period, then $\mathrm{R95p}_j = \dfrac{\sum_{w=1}^{W} RR_{wj} \text{ where } RR_{wj} > RR_{wn}95}{\text{Annual total precipitation amount}} \times 100\%$.	%
CDD	Annual maximum length of dry spell, maximum number of consecutive days with RR $<$ 1 mm Let RR_{ij} be the daily PRCP amount on day i in period j. Count the largest number of consecutive days when $RR_{ij} <$ 1mm.	days

to look for the largest (in absolute value) difference between the empirical cumulative distribution functions of samples of m_1 observations of x_1 and m_2 observations of x_2. The null hypothesis that the two data samples were drawn from the same distribution is rejected at the α 100% level if

$$D_S > \left[-\frac{1}{2}\left(\frac{1}{m_1}+\frac{1}{m_2}\right)\ln\left(\frac{\alpha}{2}\right)\right]^{1/2}, \tag{2}$$

where for a 5% level test, $\alpha = 0.05$.

b. Nonparametric Mann–Kendall test and Sen's method

The trends of the indices are estimated by the nonparametric Mann–Kendall test and Sen's method: the former one tests whether the trend is increasing or decreasing and estimates the significance of the trend, while the latter quantifies the slope of this trend.

Assume that the time series dataset obeys the model,

$$x_i = f(t_i) + \varepsilon_i, \tag{3}$$

where $f(t)$ is a monotonic increasing or decreasing function of time and the residuals ε_i can be assumed to come from the same distribution with zero mean.

When the number of data values is fewer than 10, the statistic S (Gilbert 1987) is calculated:

$$S = \sum_{k=1}^{n-1}\sum_{j=k+1}^{n} \mathrm{sgn}(x_j - x_k), \tag{4}$$

where n is the number of years; x_j and x_k are the annual values in years j and k, respectively; here $j > k$, and

$$\mathrm{sgn}(x_j - x_k) = \begin{cases} 1 & \text{if} \quad x_j - x_k > 0 \\ 0 & \text{if} \quad x_j - x_k = 0 \\ -1 & \text{if} \quad x_j - x_k < 0 \end{cases}. \tag{5}$$

If the number of years is at least 10, the normal approximation statistic Y, which is based on S from Eq. (4), will be calculated. However, the validity of Y may be reduced if there are tied values in the time series when the sample size is close to 10. Therefore, the variance of S is computed according to the equation

$$\mathrm{VAR}(S) = \frac{1}{18}\left[n(n-1)(2n+5) - \sum_{p=1}^{q} t_p(t_p-1)(2t_p+5)\right], \tag{6}$$

where q is the number of tied groups and t_p is the number of data values in the pth group.

Then the statistic Y is obtained as follows:

$$Y = \begin{cases} \dfrac{S-1}{\sqrt{\mathrm{VAR}(S)}} & \text{if} \quad S > 0 \\ 0 & \text{if} \quad S = 0 \\ \dfrac{S+1}{\sqrt{\mathrm{VAR}(S)}} & \text{if} \quad S < 0 \end{cases}. \tag{7}$$

A positive (negative) value of S or Y indicates an upward (downward) trend. The significance of the trend can be obtained from the table of the standard normal distribution cumulative probabilities.

When using the Sen's method to estimate the slope of the trend, assume that the $f(t)$ in Eq. (3) can be represented by

$$f(t) = Qt + B, \tag{8}$$

where Q is the slope to be estimated and B is a constant.

Then the slopes of all data pairs are calculated according to the equation

$$Q_i = \frac{x_j - x_k}{j - k}, \tag{9}$$

where $j > k$. The median of all these slopes of data pairs is the Sen's estimator of slope.

The advantage of these two methods is that missing values are allowed and the data need not conform to any particular distribution. Further, the Sen's method is not greatly affected by single data errors or outliers.

c. Fisher's Z transformation

When examining the significance of the correlation coefficients between indices and the Southern Oscillation index (SOI) at every station, the Fisher Z transformation (Wilks 2006) is applied to the correlation coefficients,

$$Z = \frac{1}{2}\ln\left(\frac{1+r}{1-r}\right), \tag{10}$$

where r represents the original correlation coefficient. Under the null hypothesis that the correlation r is zero, the Z approximately follows the Gaussian distribution with $\mu = 0$ and $\sigma = (n-3)^{-1/2}$, in which n is the sample size. Absolute values of Z larger than $1.645/\sqrt{n}$ would be declared significant at the 10% level and absolute values larger than $1.96/\sqrt{n}$ are significant at the 5% level. The corresponding values used to estimate the significance of the correlation coefficient can be calculated by the transformation of Eq. (10):

$$r = \frac{e^{2Z} - 1}{e^{2Z} + 1}. \tag{11}$$

d. Nonparametric Mann–Whitney U test

Nonparametric Mann–Whitney U test, also known as the Wilcoxon–Mann–Whitney rank sum test, is used to evaluate the indicator's differences between two independent data samples (Chu and Chen 2005). The null hypothesis is that the two data samples have been drawn from the same distribution. Assume that we have two batches of sample data, with sample sizes n_1 and n_2. To perform this test, the two data batches need to be pooled and ranked. Let U be the Mann–Whitney U statistic:

$$\begin{aligned} U_1 &= R_1 - \frac{n_1}{2}(n_1 + 1) \\ U_2 &= R_2 - \frac{n_2}{2}(n_2 + 1), \end{aligned} \tag{12}$$

where R_1 and R_2 are defined as the sum of the ranks held by the two batches. The null distribution of the Mann–Whitney U statistic is approximately Gaussian when n_1 or n_2 are moderately large with

$$\mu_U = \frac{n_1 n_2}{2} \quad \text{and} \tag{13}$$

$$\sigma_U = \left[\frac{n_1 n_2 (n_1 + n_2 + 1)}{12}\right]^{1/2}. \tag{14}$$

Once μ_U, σ_U, and U_1 (or U_2) are computed, the U statistic at each station is transformed into a standard Gaussian variable and is evaluated for its statistical significance.

4. Temporal and spatial characteristics of climate change indices

a. Long-term temporal characteristics

The annual probability density functions (PDFs) for all the five indices are shown in Figs. 2a–e. To see the difference in precipitation characteristics over the last six decades, the overall dataset is separated into two near-30-yr epochs: 1950–79 and 1980–2007. Because trends of the water year and those of the winter season display comparable features, only winter season statistics are provided. Figure 2a shows a pronounced drop and shift to the left in the PDF peaks from the early epoch to the recent epoch, implying the frequency of average precipitation intensity has decreased with time. From the empirical data, the average precipitation intensity can be roughly classified into three groups: light intensity being less than 10 mm day^{-1} in wet days, moderate intensity being 10–15 mm day^{-1}, and high intensity being larger than 15 mm day^{-1}. The percentage of light, moderate, and high precipitation intensity of the two periods are given in Table 3. Overall, there is a decrease of average moderate and high precipitation intensity and a concomitant increase of light precipitation intensity over time.

For R25 (Fig. 2b), the dominant feature is the shift in the distribution toward the left with time, from a less skewed distribution in the early epoch to that of a

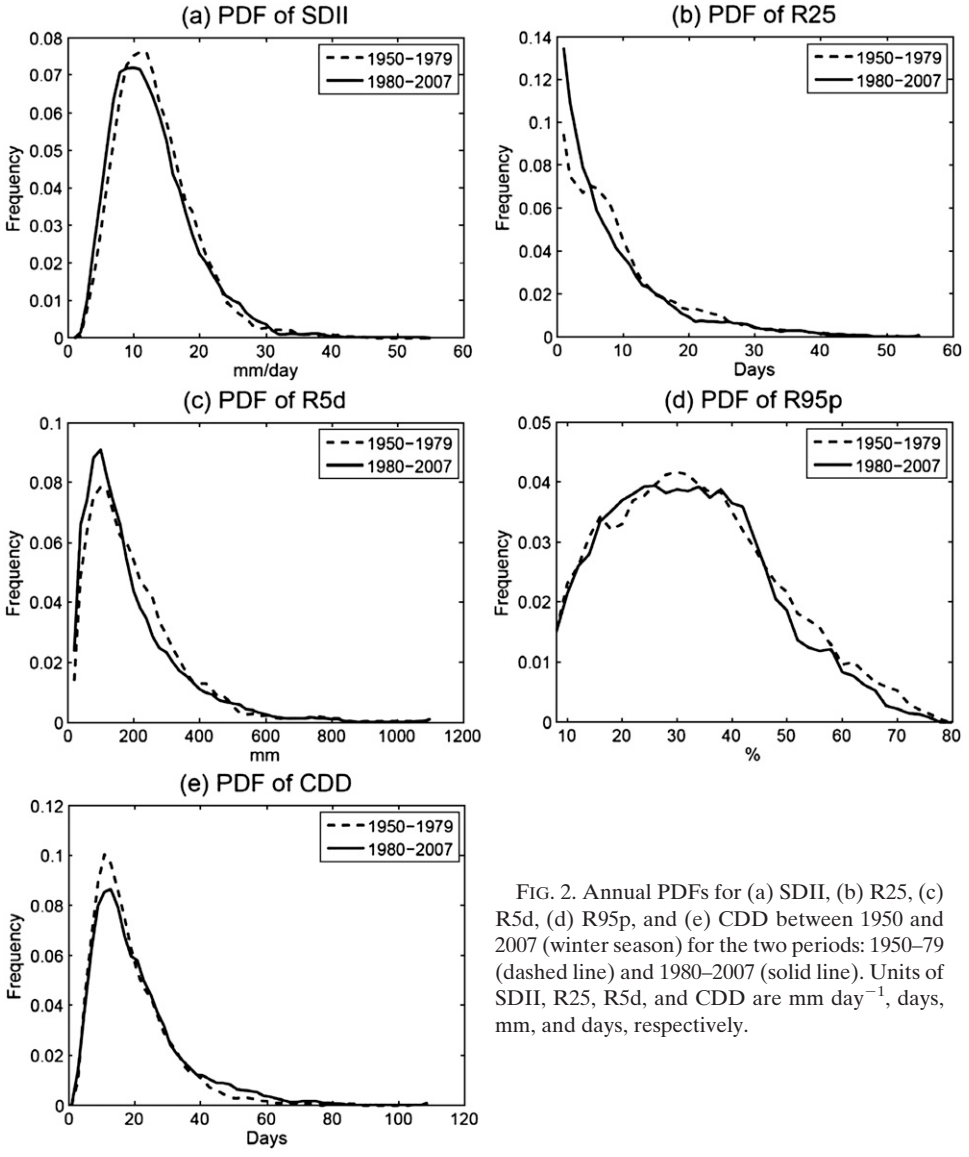

FIG. 2. Annual PDFs for (a) SDII, (b) R25, (c) R5d, (d) R95p, and (e) CDD between 1950 and 2007 (winter season) for the two periods: 1950–79 (dashed line) and 1980–2007 (solid line). Units of SDII, R25, R5d, and CDD are mm day^{-1}, days, mm, and days, respectively.

strongly skewed one in the second epoch. Specifically, the frequency of annual days with greater than 25.4 mm daily rainfall cluster in the range between 6 and 24 days has decreased from the first epoch to the second epoch. Similarly, the PDFs of R5d (Fig. 2c) display a reduction in the frequency of annual maximum consecutive 5-day precipitation amount in the range between 200 and 400 mm from the early epoch to the recent epoch. This decrease is compensated for by an increase in the peak of the distribution. The changes for R95p in Fig. 2d are less clear than the other three wetness indices; however, on the right side of the PDF, the decrease in the frequency of the fraction of annual total precipitation due to events exceeding the 95th percentile is evident from the first epoch to the recent epoch.

In summary, the shift in PDFs shown in all four wetness indicators is qualitatively consistent with Chu and Chen (2005), in which they noted a descending trend in the Hawaii rainfall index (HRI) during the last century. The monthly rainfall data from nine stations on each of the three islands—Kauai, Oahu, and the island of

TABLE 3. Percentage of light, moderate, and high PRCP intensity during the two near-30-yr periods, 1950–1979 and 1980–2007, winter season.

	1950–79 (%)	1980–2007 (%)
Light (<10 mm day^{-1})	27.08	32.94
Moderate (10–15 mm day^{-1})	44.09	39.56
High (>15 mm day^{-1})	28.83	27.50

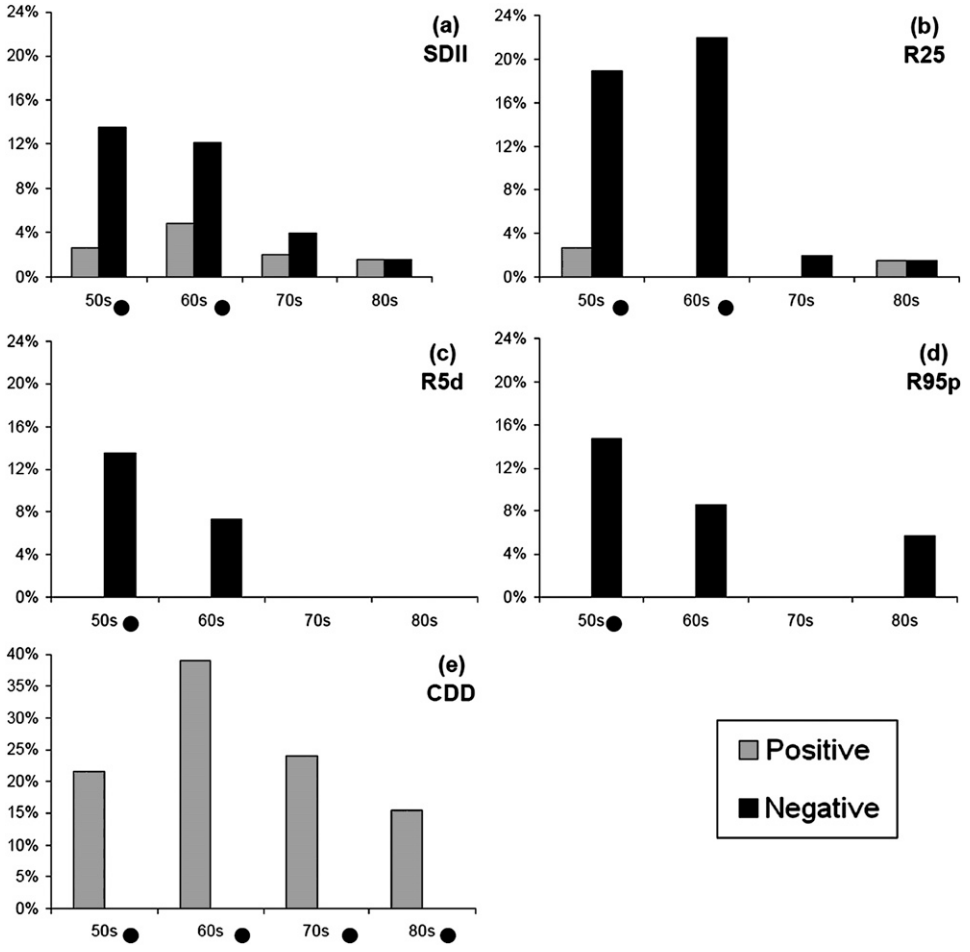

FIG. 3. Percentage of stations with positive or negative trend significant at the 10% level in different periods for each index: (a) SDII, (b) R25, (c) R5d, (d) R95p, and (e) CDD, winter season. Here 50s stands for the period from the 1950s to 2007, 60s means from the 1960s to 2007, and so on. Solid circle on the right of the time at the bottom means field significant at the 5% level.

Hawaii—were used to construct the HRI. These stations are also arranged at various elevations (i.e., high medium, and low) and different locations regarding the direction of the prevailing trade wind (i.e., windward, leeward, and neutral). HRI approximates the average conditions of monthly or seasonal Hawaii rainfall. Therefore, not only precipitation totals but also extreme precipitation in Hawaii has undergone a long-term downward shift.

As for CDD (Fig. 2e), the location of the peak for two epochs varies slightly and is found to be about 9–11 days. There is a marked decrease in the peak distribution with time. This indicates that the frequency of occurrences of the annual maximum number of consecutive dry days near the peak is smaller in the most recent period. Also note a higher percentage of occurrences on the right side of the distribution for the most recent epoch, implying that the annual maximum number of consecutive dry days from 35 to 80 days tends to occur more often in the last three decades.

While the results presented in Fig. 2 reveal qualitatively a shift of PDFs, there is a concern whether the change of the number of stations would influence the corresponding distribution of the PDFs. For this purpose, a two-sample K-S test is applied. For the period of 1980–2007, two batches of data with different station numbers are sampled. That is, one batch is based on the number of stations identical to the first epoch [i.e., sample size m_1 in Eqs. (1) and (2)] and the other batch is just the number of stations available in the recent epoch [i.e., sample size m_2 in Eqs. (1) and (2)]. For this case, the period is fixed (i.e., 1980–2007). Our results (not shown) show that for every dataset pair, the null hypothesis that they were drawn from the same distribution cannot be rejected at the 5% level. This implies that the change of station numbers, which are associated with the difference

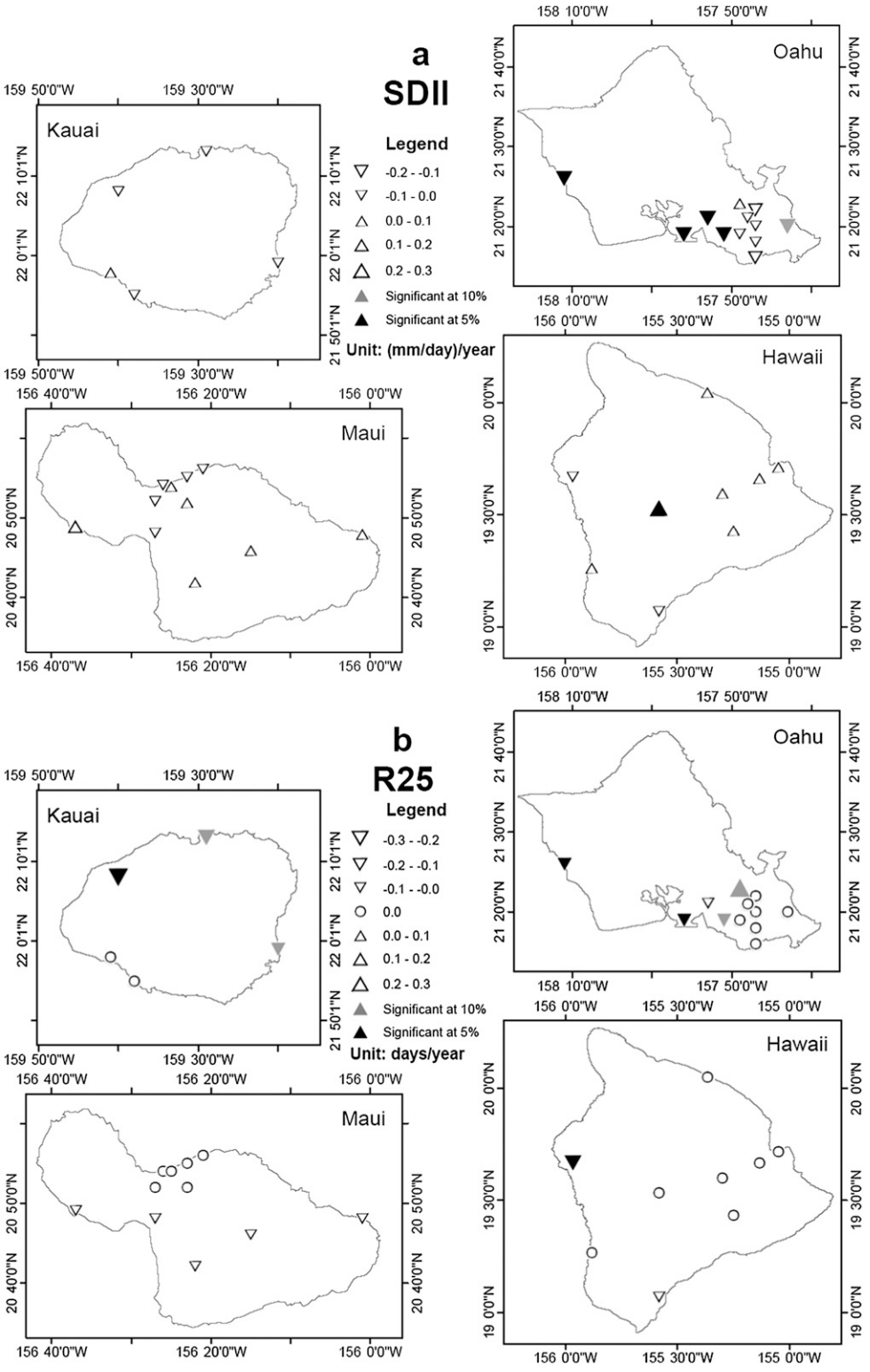

FIG. 4. Spatial pattern of Sen's slope for different indices for the period of the 1950s–2007 winter season in each grouping: (top) (left) Kauai and (right) Oahu and (bottom) (left) Maui and (right) Hawaii: (a) SDII, (b) R25, (c) R5d, and (d) CDD [values (100 yr)$^{-1}$]. Triangles and circles denote the locations of the individual stations. Upward (downward) hollow triangles indicate positive (negative) direction of trends, and their size corresponds to the magnitude of trends. Gray (black) triangles indicate trends significant at the 10% (5%) level. Units of the slopes of SDII, R25, R5d, and CDD are mm day^{-1} yr^{-1}, days yr^{-1}, mm yr^{-1}, and days yr^{-1}, respectively.

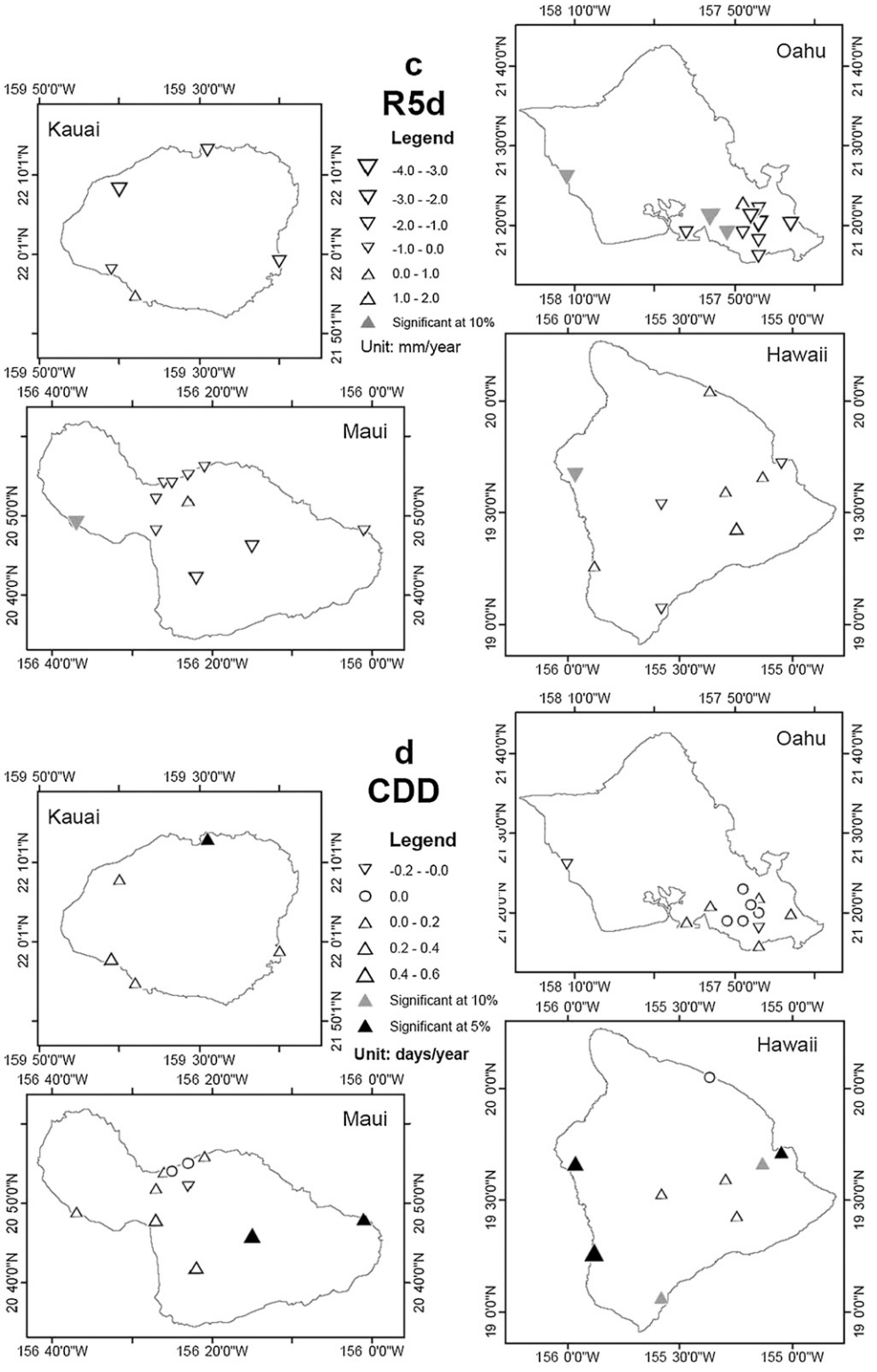

FIG. 4. (*Continued*)

in sample sizes, does not influence the underlying distribution of the dataset. The two-sample K-S test can also be used to determine whether the PDFs of the two different epochs follow the same distribution. For this test, the datasets compared are two different periods (1950–79 verses 1980–2007). Results from the K-S test indicate that for all the five indicators, except R95p, the null hypothesis can be rejected at the 5% level, which means there are significant changes in the distributions from one epoch to another.

As aforementioned, there are significant shifts in the statistical distributions of four of the five indicators. To better understand the long-term fluctuations in precipitation extremes, a nonparametric trend analysis is applied to records of varying length, as trend statistics are sensitive to the time windows chosen. If the statistical significance is not considered, then a large percentage of stations (60%–80%) would show downward trends in precipitation-related indices corresponding to various periods and upward trends for CDD. The percentages of stations with significant positive and negative trends corresponding to various periods for all five indices are given in Fig. 3. In the trend analysis, the last year is fixed to be 2007 but the starting year is not because each station begins its observation differently. Instead of using the same starting year, which would limit the number of gauges used, we use, say, the 1950s for all gauges that show records starting in the 1950s. Hence, the 1950s stand for the period from the 1950s to 2007, and the 1960s represent the period from the 1960s to 2007, and so on (Fig. 3). This is consistent with the U.S. Geological Survey report about trends in streamflow characteristics (Oki 2004).

In a given dataset, one would expect a certain number of stations or grids to pass a significant test at random. To ensure the significance at individual stations is not due to random chance, multiple testing is performed to investigate the field significance (the so-called multiplicity problem). That is, it is also necessary to address the collective significance of a finite set of individual significance tests for the entire field (Chu and Wang 1997). Assuming spatial independence, a binomial probability distribution can be used to evaluate the overall significance of the trends (Wilks 2006).

From the 1950s to 2007 or from the 1960s to 2007, for all four indices associated with precipitation extremes, including SDII, R25, R5d, and R95p (Figs. 3a–d), downward trends prevail. Take SDII as an example (Fig. 3a). For the periods from the 1950s to 2007 and from the 1960s to 2007, about 13% of the stations have significant negative trends, while only around 4% show significant positive trends. This feature slightly becomes more pronounced in R25 (Fig. 3b), which is related to the frequency of intense precipitation events. From the 1950s to 2007, approximately 20% of the stations are characterized by significant negative trends. Moreover, significant negative trends are predominant from the 1960s to 2007, as almost 22% of stations (e.g., nine stations) fall into this category (Fig. 3b). Similarly, for the two indices associated with the magnitude of most intense precipitation events (i.e., R5d and R95p), the percentage of significant negative trend in R5d reaches about 14% (Fig. 3c) and about 15% for R95p from the 1950s to 2007 (Fig. 3d). This suggests that for some stations in Hawaii, extreme precipitation has experienced a significant long-term downward trend. Results from multiple testing suggest that all the downward trends from the 1950s to 2007 reach field significance for all four indices, and from the 1960s to 2007, two indices (SDII and R25) achieve field significance.

Another salient feature in Fig. 3 is the decrease of the percentages of significant negative trends from the earlier epoch to the latter epoch. In other words, in the more recent decades, stations are inclined to exhibit fewer negative trends or the percentages of positive and negative trends tend to be comparable. This transition appears to occur around the period in the 1970s (Figs. 3a–c). Interestingly, this occurs in the presence of a long-term downward trend in precipitation extremes since the 1950s. Note that the aforementioned positive and negative trends since the 1970s do not reach field significance according to multiple testing. However, as the analysis period shortens, unforced natural variability becomes a greater factor when considering trends; more research needs to be done to investigate this feature.

The CDD, which represents drought conditions, shows significant positive trends for all periods, and the trends of all the periods reach field significance (Fig. 3e). One noteworthy feature is a gradual drop in the percentage of the significant positive trends in the last two periods. As discussed earlier, whether this suggests that there are fewer areas with longer annual maximum consecutive dry days since the 1970s needs to be studied in the future.

b. Long-term spatial characteristics

As mentioned in section 4a, the temporal characteristics suggested that the four precipitation-related indices—SDII, R25, R5d, and R95p—displayed long-term downward trends, and the index related to drought—CDD—showed a long-term upward trend. To obtain a better understanding regarding which station or area experiencing these features, the spatial layout of trends is analyzed.

1) CLIMATOLOGY AND INTERANNUAL VARIATIONS OF RAINFALL IN HAWAII

Before looking into the spatial features of the indices trend, it is instructive to review the climatological mean

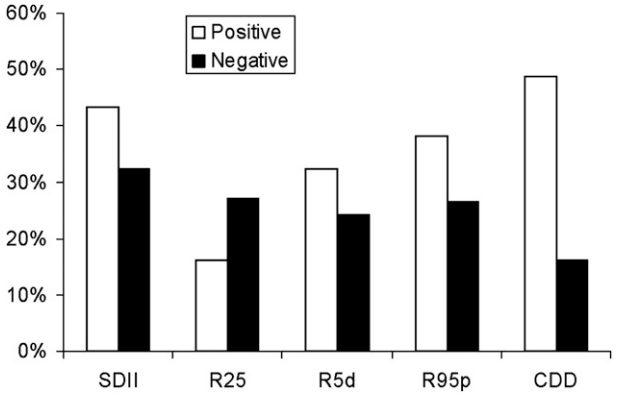

FIG. 5. Percentage of stations with positive or negative derivatives of the trends for 30-yr running series significant at the 10% level for SDII, R25, R5d, R95p, and CDD, winter season. All the derivatives of the trends are field significant at the 5% level.

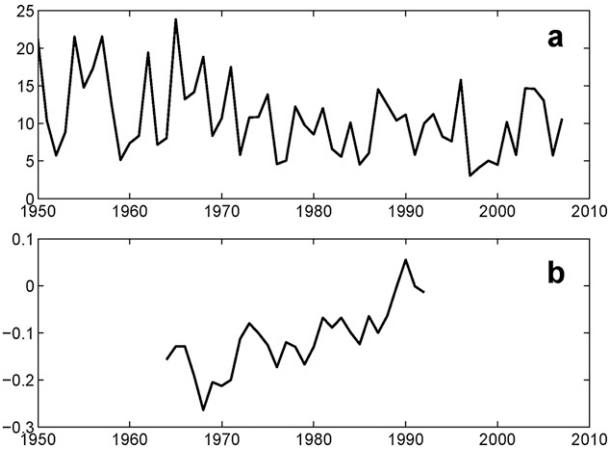

FIG. 6. Time series of SDII (a) in mm day^{-1} and (b) trends derived from the 30-yr running series in mm day^{-1} yr^{-1} at Honolulu International Airport. The numbers on the x axis locates the middle of the period, for example, 1964 represents 1950–79, 1965 represents 1951–80.

precipitation pattern and interannnual rainfall variations in the Hawaiian Islands. Hawaii climatological mean annual rainfall maps (Blumenstock and Price 1967; Giambelluca et al. 1986) suggest that maximum rainfall centers are located at lower elevations (approximately 600–1200 m) along the windward slope of high mountains such as Mauna Kea, whose elevation exceeds 4100 m (Fig. 1). Thermally forced diurnal circulations, including land–sea breezes and mountain–valley winds, contribute to rainfall development in this region by enhancing orographic uplifting of the trade winds from the open ocean and inducing low-level convergence with the trades (Leopold 1949; Chen and Nash 1994). As a result, high rainfall is commonly found along the lower portion of the eastern flanks of Mauna Kea such as near Hilo, known as one of the wettest cities in the United States. At high elevations well above the trade inversion that acts as a lid to vertical motion and convection, arid climate prevails. The southeastern flank of Mauna Loa is vulnerable to synoptic disturbances and thus is marked by a secondary maximum rainfall center. During the cool season, southeasterly winds associated with synoptic systems may bring heavy rainfall to this region (Kodama and Barnes 1997). For mountains with moderate heights but below the trade wind inversion that usually occurs at 2 km (Cao et al. 2007), maximum rainfall centers are found near their summit (Schroeder 1977; Ramage and Schroeder 1999). These include the West Maui Mountains, the Koolau Range of Oahu, and Mt. Waialeale on Kauai (Fig. 1). The overall rainfall pattern in Hawaii is marked by the windward wet and leeward dry. This dryness is also known as rain shadow effect and is most pronounced on the island of Hawaii.

Precipitation in Hawaii is sensitive to ENSO. Previous research has suggested the relationship between Hawaiian winter precipitation anomalies and ENSO (Lyons 1982; Taylor 1984; Chu 1989; Cayan and Peterson 1989). A mechanism that associates deficient precipitation in Hawaii during winter with El Niño was proposed by Chu (1995), who highlighted the effect of the upper-tropospheric jet stream on Hawaii precipitation. Chu and Chen (2005) further suggested that Hawaii precipitation is also modulated by the PDO. When the El Niño event is embedded in the positive phase of the PDO, precipitation in Hawaii is greatly reduced, while the occurrence of La Niña during the negative phase of the PDO contributes to more abundant precipitation.

2) SPATIAL PATTERN OF TRENDS FROM THE 1950S TO 2007

As illustrated in Fig. 3, when there is a trend in precipitation extremes, it is most often downward. Here, we will demonstrate the geographic distribution of trends in indices for four major Hawaiian Islands for the periods of the 1950s–2007. The Sen's method is used to estimate the slope of the trends and only the winter season is displayed. The significance of the trends is assessed from the results of the Mann–Kendall method. Because R5d and Q95p both represent the magnitude of the extreme precipitation, for the sake of simplicity, only SDII, R25, R5d, and CDD are provided for the period chosen.

Figure 4a shows the trend pattern for SDII. For Kauai, an insignificant decreasing trend in average precipitation intensity is found in the relatively wet northern portion of the island, where the historical mean annual precipitation ranges from 1500 to 3000 mm. For the relatively dry western portion, where the mean annual precipitation ranges from 500 to 1000 mm, an insignificant

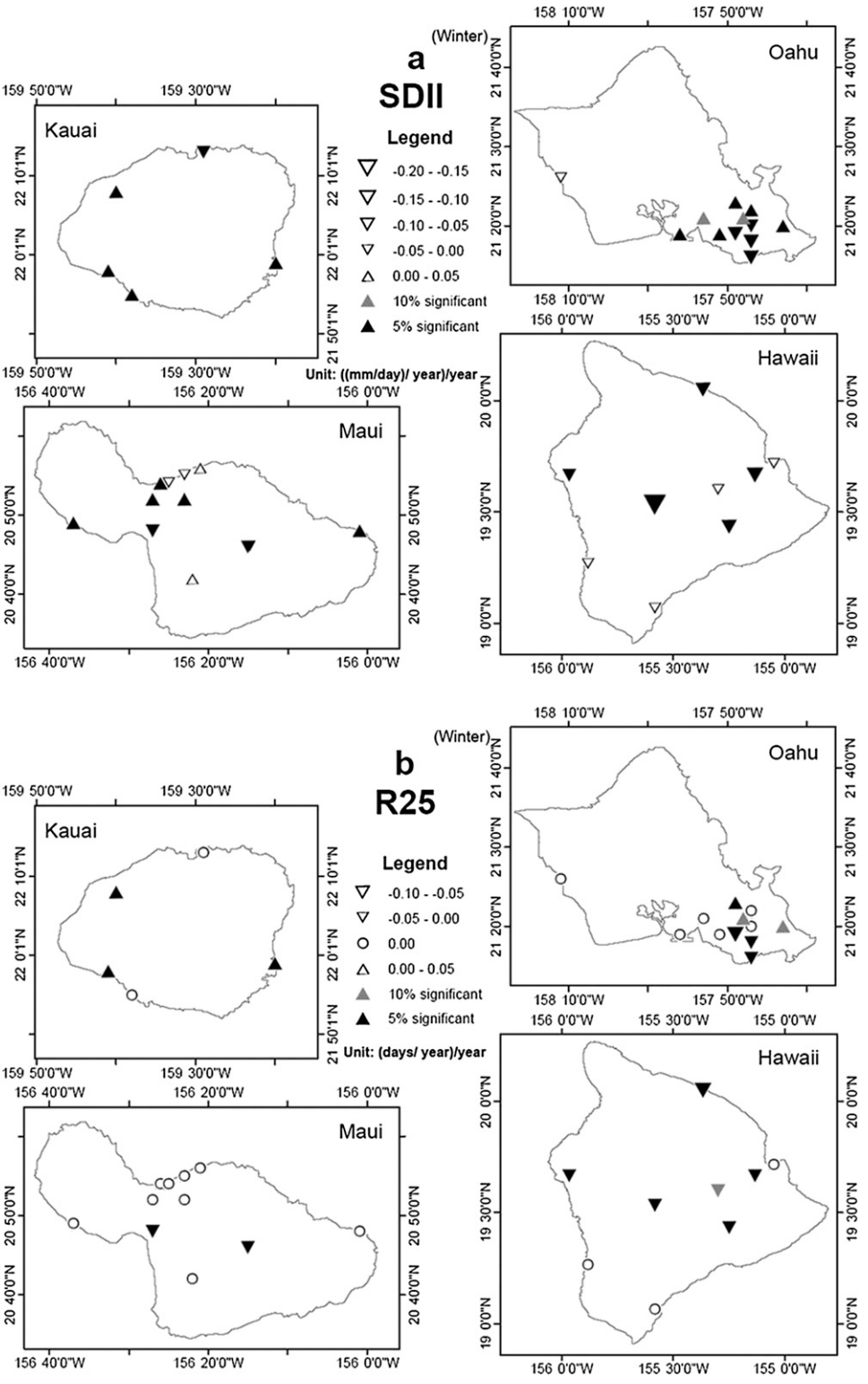

FIG. 7. As in Fig. 4, but for derivatives of the trends of 30-yr running series for the periods from 1950–79, 1951–80, . . . , to 1978–2007.

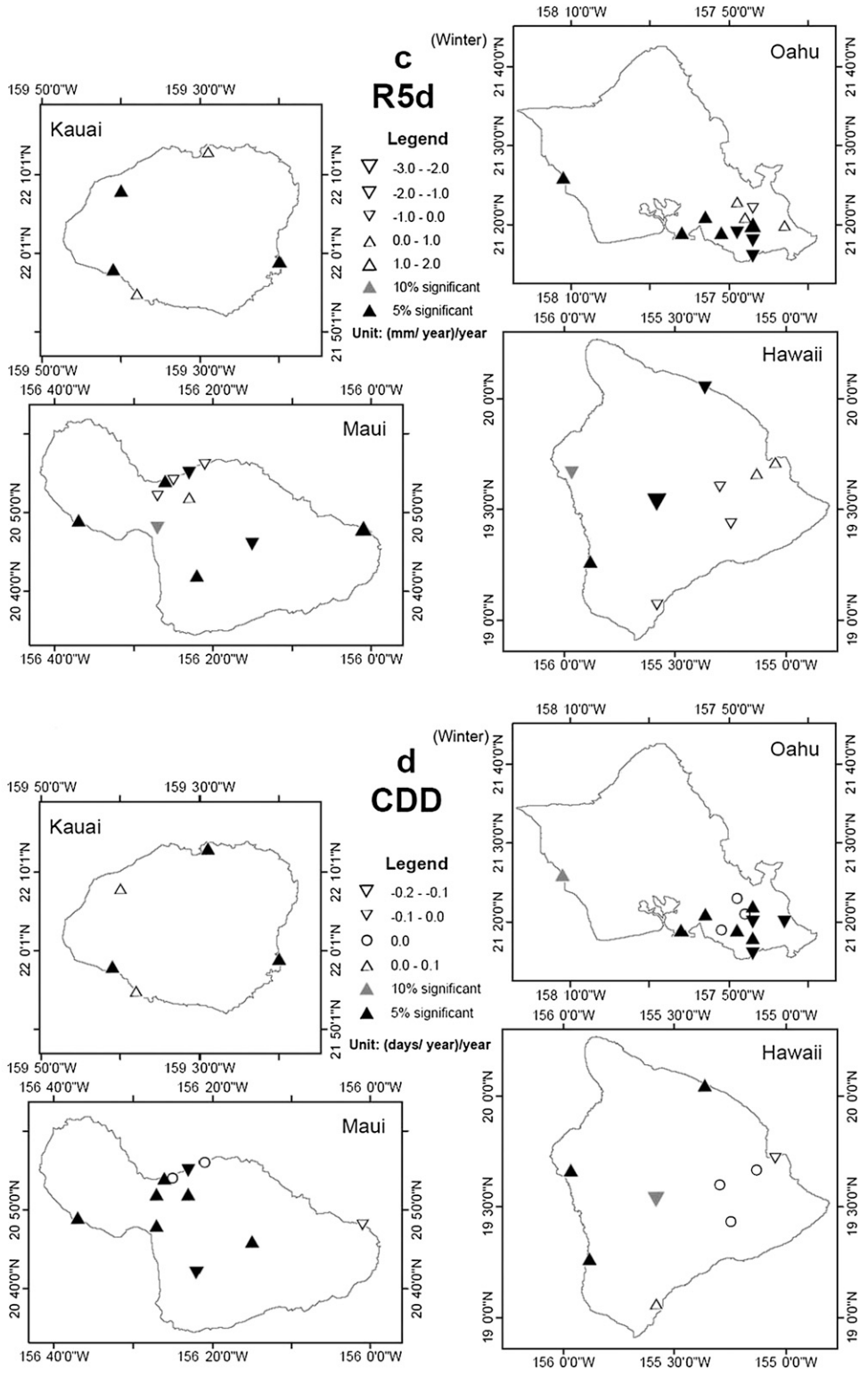

FIG. 7. (*Continued*)

increasing trend is noted in one station and decreasing in another. Therefore, at lower elevations of Kauai, precipitation became less intense in the wet northern coast since the 1950s, while there is no clear trend in the dry western coast. Because there is no station that meets our criteria (defined in section 2a) on the summit Waialeale, which is in central Kauai and the wettest spot of all the Hawaiian Islands, the tendency there is not clear.

The most pronounced feature of precipitation intensity on Oahu is the prevailing downward trend (Fig. 4a). Except for one station near the eastern Koolau Range, all the other stations exhibit a decreasing trend. In the Manoa Valley area (Fig. 1), where a secondary maximum mean annual precipitation center with value ranging from 3000 to 4000 mm is noted, the downward trend is insignificant. This area also coincides with the centers of heavy and very heavy precipitation events (Chu et al. 2009). For the south-facing leeward coast of Oahu, including Punchbowl Crater, Fort Shafter, and Honolulu International Airport, a significant downward trend is noticeable (Fig. 4a). This region is characterized not only by low mean annual precipitation ranging from 500 to 1000 mm but also lower precipitation intensity associated with a specific return period (Chu et al. 2009). For the lone station in western Oahu (Waianae), where mean annual precipitation is below 600 mm, the downward trend is also significant.

The insignificant negative trend in central Maui is flanked by insignificant positive trends on both sides (Fig. 4a). In Hana and the Mt. Haleakala area of Maui, an upward trend is seen. The passage of midlatitude systems and topographic forcing caused by Mt. Haleakala are able to trigger heavy precipitation events in Hana (Lyman et al. 2005). The lack of stations on West Maui Mountain, where the mean annual precipitation is high, precludes the confirmation of a trend there. For the island of Hawaii (Fig. 4a), the predominant characteristic is positive trends in precipitation intensity, which extends from Hamakua to Puna, with a significant positive trend center located around the summit of Mt. Mauna Loa. The negative trends, on the other hand, are seen in stations around Kona and the southern part of the island of Hawaii.

The patterns for the trends of R25 are given in Fig. 4b, and negative trends are dominant in all the four major islands of Hawaii. For Kauai, as similar to SDII (Fig. 4a), the frequency of intense precipitation events, defined as the annual number of days with daily precipitation greater than 25.4 mm, exhibits a significant decreasing trend in the wet northern region, while no trend is found in the dry western coast. For Oahu (Fig. 4b), significant downward trends in the south-facing leeward coast and the west are noted. There is a single station in the Koolau Range with a significant upward trend. This spatial pattern is similar to the corresponding one in precipitation intensity (Fig. 4a). When R25 is large, indicative of more intense precipitation days, it would likely result in more total precipitation amounts on wet days. Because SDII is a metric for precipitation rate, the average precipitation intensity on wet days would be larger and correspond to that in R25. In Fig. 4b, Maui is dominated by insignificant negative trends since the 1950s. For the island of Hawaii, there are a large number of stations with no trend (i.e., the Sen's slope equals to zero) and a single station in the Kona area with significant negative trend.

The spatial pattern for trends of R5d, a rough proxy of extreme precipitation magnitude accumulated over a 5-day period in a year, is found in Fig. 4c. Consistent with Figs. 4a,b, northern Kauai has experienced an insignificant decreasing trend in R5d (Fig. 4c). For Oahu, the majority of the stations display downward trends, and this feature is qualitatively similar to the corresponding Oahu maps shown in Figs. 4a,b. Significant downward trends are found for two stations in the south-facing coast and one in western Oahu (Fig. 4c). For Maui, the downward trends in extreme precipitation magnitude prevail at almost all the stations. For the island of Hawaii, the pattern is mixed and a significant negative trend is noted around Kona.

Recall that during all the periods, upward trends in CDD prevail (Fig. 3e); that is, most stations are characterized by positive trends in the annual maximum consecutive dry days regardless of the chosen time windows. This is corroborated by Fig. 4d, in which all major Hawaiian Islands have experienced increasing trends. There are five stations showing significant upward trends at the 10% level or higher on the island of Hawaii, two on Maui, and one on Kauai.

In summary, since the 1950s, for Kauai, not only average daily precipitation intensity but also intense precipitation frequency and magnitude decreased over the areas where the climatological mean precipitation is relative abundant (Figs. 4a–c). Therefore, climate extremes have become less extreme for Kauai since the 1950s. For Oahu, there is also an indication that the aforementioned precipitation attributes decreased over the dry areas. For the island of Hawaii, the situation is somewhat different, with more stations in wet regions tending to show upward trends, while downward trends have been seen in dry areas. The southeastern-most position and highest elevation make the precipitation trends in this island to be different from the others. For the duration of dryness, most islands exhibit a tendency to have longer, consecutive periods of no precipitation days since the 1950s (Fig. 4d).

c. *Temporal and spatial characteristics of derivatives of trends from 30-yr running series*

The discussion in sections 4a and 4b provided the temporal and spatial features of the long-term downward trends in precipitation-related indices and upward trend in the drought index from the 1950s to 2007. To better understand the temporal behavior of trends of the indices in Hawaii, 30-yr running series are selected; that is, time-dependant changes in extreme precipitation events are examined for a 30-yr interval, but the series are moving forward 1 yr at a time (i.e., starting from 1950 to 1979, 1951 to 1980, until 1978 to 2007). As such, 29 series, each of which encompasses a fixed 30-yr period, are constructed for every index at each station. The 30-yr running series allows temporal changes in the extremes to be evaluated in more detail (e.g., DeGaetano 2009). The trends of every 30-yr interval are calculated using the Mann–Kendall test and Sen's method. Having done that, the derivative of the trends, which is derived from the trends of the individual 30-yr running series, are assessed again using the Mann–Kendall test and Sen's method. By doing this, it would allow us to investigate whether the aforementioned trends are stable or changing in time. A direction of the trend is deemed stable if the long-term upward (downward) trend is accompanied by a positive (negative) derivative of the trend. On the other hand, it is changing in time (e.g., the trend becomes gentle or even changes sign) when the upward–downward long-term trend acts in the direction opposite to the derivative of the trend.

In Fig. 5, the percentages of significant positive (or negative) derivatives of trends of 30-yr running series are given, with more stations having positive derivatives for three out of the four indices related to precipitation extremes. Specifically, about 45% of the stations show significant positive derivatives in average daily precipitation intensity (SDII), and 33% and 40% in the magnitude of significant precipitation, R5d and R95p, respectively. Because some stations exhibit significant long-term downward trends (Fig. 3), results from Fig. 5 suggest a slowdown of the decreasing trend with time or even a sign shift toward an upward trend. This is exemplified by the precipitation extremes at the Honolulu International Airport, Oahu. For the time series of SDII, it is obvious that the precipitation intensity dropped in the long run (Fig. 6a); however, the slope of the decreasing trend slowed down or even reversed since the 1980s. As a result, the time series of trends of 30-yr running series become less negative or even turn to positive, leading to a positive derivative (Fig. 6b). For R25 (Fig. 5), more stations are characterized by significant negative derivatives than by positive derivatives. This is probably due to the definition of R25. For relatively dry areas, annual total numbers of days with daily precipitation amounts greater than 25.4 mm day^{-1} are rare. Without a sufficient number of cases, the trends of every 30-yr series are small or negligible, which in turn lead to zero derivatives of the trends. Therefore, caution must be taken when interpreting the result for R25. As for CDD (Fig. 5), which represents the drought condition, there is a prevailing positive derivative. Because CDDs have long-term increasing trends (Fig. 3), these suggest that the annual maximum consecutive no-precipitation days tend to increase and this change is stable with time.

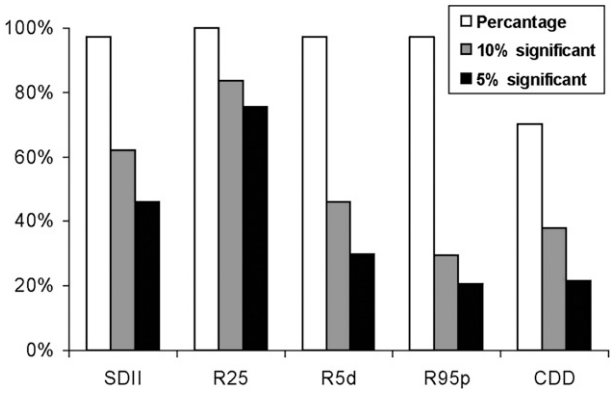

FIG. 8. Percentage of stations having positive correlations between indices and the SOI and negative correlations between CDD and the SOI.

The spatial patterns of the derivatives of trends of 30-yr running series for the indices are given in Fig. 7. The most noteworthy feature is the prevalence of positive derivatives of trends in Kauai and Oahu, but negative derivatives on the island of Hawaii. Take SDII as an example. Three out of the four stations in Kauai that displayed insignificant long-term downward trends in Fig. 4a now show significant positive derivatives based on the 30-yr running series (Fig. 7a). Significant positive derivatives can also be found in many stations in Oahu, especially in those stations where the long-term trends are significantly downward. The dominance of positive derivatives in central Maui is noticeable too. Different from Oahu and Kauai, the most noteworthy feature on the island of Hawaii is the prevalence of negative derivatives. Because most stations demonstrated long-term upward trends (Fig. 4a), the negative derivative in Fig. 7a implies a sign change for the island of Hawaii.

As for R25, the most salient pattern is positive derivatives in Kauai and negative derivatives prevail on the island of Hawaii (Fig. 7b). For R5d (Fig. 7c), the resulting pattern is similar to that of SDII (Fig. 7a), with significant positive derivatives dominating Kauai and Oahu and negative ones are noted on the island

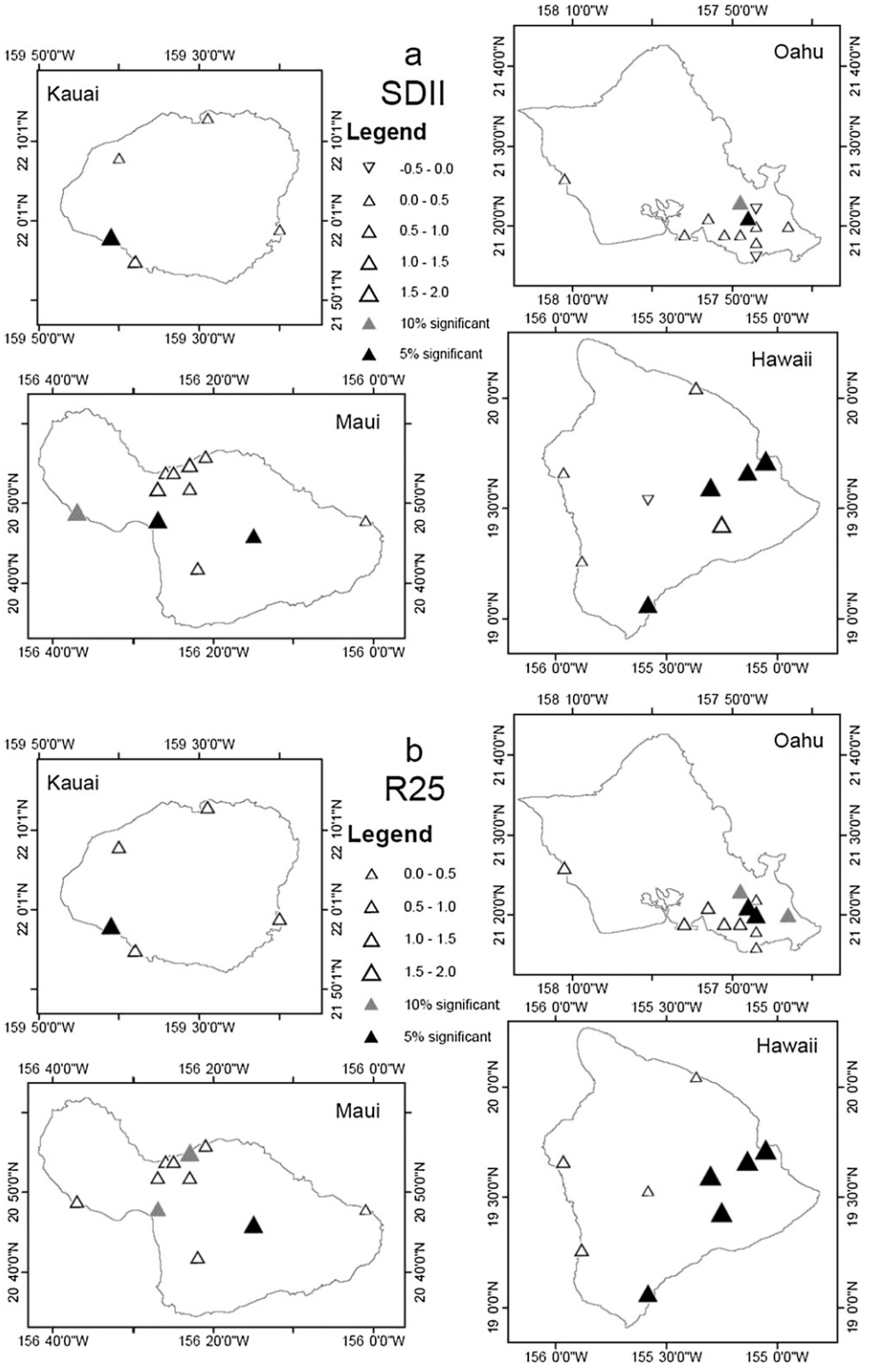

FIG. 9. Composites of standardized anomalies of indices in each grouping: (top) (left) Kauai and (right) Oahu and (bottom) (left) Maui and (right) Hawaii. (a) SDII, (b) R25, (c) R5d, and (d) CDD using La Niña/−PDO minus El Niño/+PDO. Upward (downward) triangles indicate positive (negative) anomalies, and their size shows magnitude of the anomalies. Gray (black) triangles indicate trends significant at the 10% (5%) level, respectively.

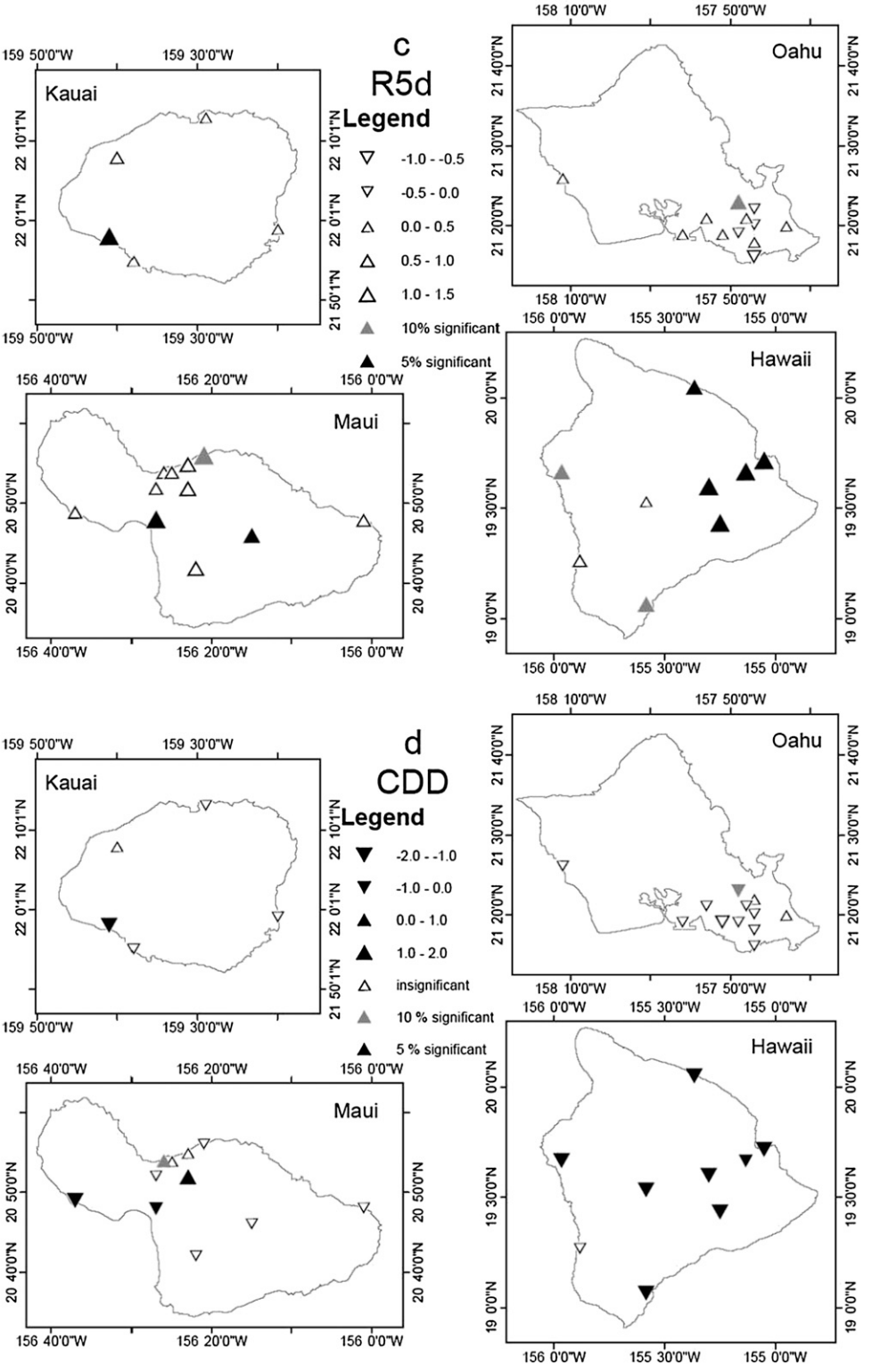

FIG. 9. (*Continued*)

of Hawaii. Considering derivatives of trends in CDD (Fig. 7d), the major Hawaiian Islands are marked by positive derivatives.

To sum up, although there are long-term downward trends for most stations in Kauai and Oahu, the derivatives of these trends from the 30-yr running series are showing the opposite direction. This suggests more extreme precipitation events recently for Oahu and Kauai. On the contrary, long-term upward trends but with negative derivatives are found in many of the stations on the island of Hawaii (e.g., Figure 7a). For CDD, trends derived from the 30-yr running series suggest that the island of Hawaii tends to have longer consecutive dry days since the 1950s and the trend is stable through time.

5. Relationship between climate change indices and ENSO/PDO

Former studies have analyzed the relationship between Hawaiian precipitation and ENSO. Chu (1995) and Chu and Chen (2005) proposed a mechanism that could result in the deficient precipitation during El Niño winters in Hawaii. To determine whether this relationship exists between extreme events and ENSO, the correlation between each of five indices and the SOI is examined. The significance of correlations is estimated by the Fisher Z transformation.

The percentages of stations having positive (negative for CDD) correlation between indices and the SOI are given in Fig. 8. It is evident that positive correlations prevail in rainfall-related indices (SDII, R25, R5d, and R95p), with all four indices having more than 95% of stations exhibiting a positive relationship with the SOI. Furthermore, for all these four indices, about 30%–80% of the stations are significant at the 10% test level and 20%–75% of stations at the 5% level. Accordingly, when the SOI is large and positive, corresponding to a La Niña event, Hawaii not only tends to have more total precipitation but also receives more frequent heavy precipitation. For the El Niño years, when the SOI is large and negative, there are fewer extreme precipitation events. For CDD, 70% of stations are marked by negative correlations with the SOI, 37% of stations significant at the 10% level and 22% at the 5% level. This implies that during a La Niña event, the annual maximum dry days in Hawaii tend to be shorter, while they are longer for El Niño years.

To further examine the relationship between precipitation extremes and ENSO/PDO, the composite figures of standardized anomalies of the indices using La Niña/−PDO minus El Niño/+PDO are presented in Fig. 9. The PDO is in the negative phase from 1950s to 1976 and in the positive phase from 1977 to 1999. Then it became negative. From 1950 to 2007, six El Niño and eight La Niña events are chosen to make the composite. The El Niño events selected are 1976/1977, 1982/1983, 1986/1987, 1991/1992, 1994/1995, and 1997/1998; the La Niña events used are 1950/1951, 1954/1955, 1955/1956, 1970/1971, 1973/1974, 1974/1975, 1975/1976, and 2007/2008. When the differences for indices between ENSO/PDO composites are considered, the statistical significances of these differences are tested by the nonparametric Mann–Whitney test.

The composite difference in extreme precipitation indices between El Niño/+PDO events and La Niña/−PDO events is shown in Fig. 9. Generally speaking, positive anomalies are prevalent on the major Hawaiian Islands for all the precipitation-related indices (Figs. 9a–c), and most of them are significant at the 10% level or higher. As for CDD (Fig. 9d), negative anomalies prevail on all the major Hawaiian Islands except Oahu, implying the significance of the composites is not as dominant as those for precipitation-related indices there. That is to say, the relationship between CDD and ENSO/PDO in Oahu is not as strong as those between precipitation-related indices and ENSO/PDO.

6. Conclusions

For the first time, five climate change indices for extreme precipitation (four related to wetness and one related to dryness) in Hawaii have been calculated using the NCDC COOP station data. To keep the wet season data intact, water year (July–June of the next year) and winter season (November–April) are applied here. Annual probability density functions of precipitation-related indices for two different epochs (i.e., 1950–79 and 1980–2007) show a reduction in the probability of moderate and high precipitation intensity accompanied by an increase in light intensity, shorter annual total number of days with daily precipitation greater than 25.4 mm, and smaller annual maximum consecutive 5-day precipitation amounts from the first epoch to the second epoch. For the dryness indicator (i.e., CDD), the right tail of the distribution becomes heavier in the recent epoch, implying a lengthening of annual maximum number of consecutive dry days.

Using the Mann–Kendall test and Sen's method, trends of water year and winter season of various periods have been investigated to further understand the long-term variations of those indices. Long-term downward trends are noted for precipitation-related indices and upward trend for drought-related index from the 1950s to the present. One of the most salient features regarding the spatial pattern of the long-term trends is the predominance of downward trends in Kauai and

Oahu and upward trends on the island of Hawaii for the precipitation-related indices. For CDD, the most noteworthy feature is the prevalence of upward trends on all the major Hawaiian Islands.

To investigate whether the long-term trends are stable through time, time-dependent changes in precipitation extremes are examined based on a 30-yr running series. For the four indices related to precipitation, the derivatives of the trends are predominantly positive and these occur in the presence of the long-term downward trends. This is most evident in Kauai and Oahu, and it suggests that the sign in the trends is changing with time. There is an indication of more extreme precipitation events recently for Oahu and Kauai. The occurrence of negative derivatives under the background upward trends is evident on the island of Hawaii and also implies a sign change. Alternatively, the long-term upward trends of CDD is accompanied by positive derivatives, meaning that the annual maximum length of no-precipitation days has a tendency to be longer and this change is stable over time.

It is noted that extreme precipitation in Hawaii is positively associated with the SOI, and this relationship is similar to that between the statewide Hawaii rainfall index and the SOI (Chu and Chen 2005). The positive correlations between wetness indices and the SOI indicate that Hawaii tends to have abundant rainfall and more extreme precipitation events in La Niña years, while there are fewer extreme precipitation events for El Niño years. Composites of standardized anomalies of indices, based on the La Niña/−PDO minus El Niño/+PDO events, are consistent with the correlation results. The CDD, on the other hand, shows negative correlations with the SOI, implying the annual maximum length is shortened in La Niña years and lengthened in El Niño years.

The IPCC AR4 on climate change has attracted global attention. Adopting the indices widely used by the IPCC to analyze extreme precipitation in Hawaii, the current study can be used as a supplement to understanding regional climate change, especially about changes in extreme events in a warming world. We note that in regions where there has been a secular downward trend in total precipitation, such as Hawaii, noteworthy decreases have been observed in extreme precipitation events as well. However, a sign change of this long-term downward trend has been noted. Given a physical linkage between the intensification of precipitation events, the increasing of water vapor in the atmosphere, air temperature, and circulation strength in a warming background (Meehl et al. 2000; Allen and Ingram 2002; Pall et al. 2007), the upward shift of extreme precipitation in some Hawaiian Islands should not be viewed as a surprise.

Because substantial social and economic damage is often caused by extreme weather events, a thorough analysis of their changes, especially of extreme precipitation, may guide local governments or other organizations for appropriate decision making. For example, the sign change of extreme precipitation events in Hawaii is useful for its Department of Land and Natural Resources and some private owners on the assessment of dam safety and other high-hazard structures as the climate is changing. This study also complements the recent precipitation frequency study by Perica et al. (2009) and Chu et al. (2009), so that state and county agencies can better prepare their planning for flood hazards within watersheds when climate change is incorporated.

Acknowledgments. This project was partially funded by the National Park Service Task Agreement J80800700008 and by Cooperative Agreement NA090AR4320075 between the Joint Institute for Marine and Atmospheric Research (JIMAR) and the National Oceanic and Atmospheric Administration (NOAA). Thanks are due to Di Henderson and May Izumi for their editorial assistance. Discussion with Mohammad Safeeq on the trend analysis was useful. Constructive criticisms from two anonymous reviewers helped to greatly improve the presentation of this paper.

REFERENCES

Alexander, L. V., and Coauthors, 2006: Global observed changes in daily climate extremes of temperature and precipitation. *J. Geophys. Res.,* **111,** D05109, doi:10.1029/2005JD006290.

Allen, M. R., and W. J. Ingram, 2002: Constraints on future changes in climate and the hydrologic cycle. *Nature,* **419,** 224–232.

Blumenstock, D., and S. Price, 1967: Hawaii. Climates of the States. Climatology of the United States Series 60-51, U.S. Weather Bureau, 27 pp.

Cao, G., T. W. Giambelluca, D. E. Stevens, and T. A. Schroeder, 2007: Inversion variability in the Hawaiian trade wind regime. *J. Climate,* **20,** 1145–1160.

Cayan, D. R., and D. H. Peterson, 1989: The influence of North Pacific atmospheric circulation on streamflow in the west. *Aspects of Climate Variability in the Pacific and the Western Americas, Geophys. Monogr.,* Vol. 55, Amer. Geophys. Union, 375–397.

Chen, Y.-L., and A. J. Nash, 1994: Diurnal variation of surface airflow and rainfall frequencies on the island of Hawaii. *Mon. Wea. Rev.,* **122,** 34–56.

Chu, P.-S., 1989: Hawaiian drought and Southern Oscillation. *Int. J. Climatol.,* **9,** 615–631.

——, 1995: Hawaii rainfall anomalies and El Niño. *J. Climate,* **8,** 1697–1703.

——, and J.-B. Wang, 1997: Recent climate change in the tropical western Pacific and Indian Ocean regions as detected by outgoing longwave radiation records. *J. Climate,* **10,** 636–646.

——, and H. Chen, 2005: Interannual and interdecadal rainfall variations in the Hawaiian Islands. *J. Climate,* **18,** 4796–4813.

——, X. Zhao, Y. Ruan, and M. Grubbs, 2009: Extreme rainfall events in the Hawaiian Islands. *J. Appl. Meteor. Climatol.,* **48,** 502–516.

DeGaetano, A. T., 2009: Time-dependent changes in extreme-precipitation return-period amounts in the continental United States. *J. Appl. Meteor. Climatol.,* **48,** 2086–2099.

Frich, P., L. V. Alexander, P. Della-Marta, B. Gleason, M. Haylock, A. M. G. Klein Tank, and T. Peterson, 2002: Observed coherent changes in climatic extremes during the second half of the twentieth century. *Climate Res.,* **19,** 193–212.

Giambelluca, T. W., M. A. Nullet, and T. A. Schroeder, 1986: Rainfall atlas of Hawaii. Division of Water and Land Development, State of Hawaii, Tech. Rep. R76, 267 pp.

——, H. F. Diaz, and M. S. A. Luke, 2008: Secular temperature changes in Hawai'i. *Geophys. Res. Lett.,* **35,** L12702, doi:10.1029/2008GL034377.

Gilbert, R. O., 1987: *Statistical Methods for Environmental Pollution Monitoring*. Wiley, 320 pp.

Griffiths, M. L., and R. S. Bradley, 2007: Variations of twentieth-century temperature and precipitation extreme indicators in the northeast United States. *J. Climate,* **20,** 5401–5417.

Kharin, V. V., and F. W. Zwiers, 2000: Changes in the extremes in an ensemble of transient climate simulations with a coupled atmosphere–ocean GCM. *J. Climate,* **13,** 3760–3788.

Klein Tank, A. M. G., and G. P. Können, 2003: Trends in indices of daily temperature and precipitation extremes in Europe, 1946–99. *J. Climate,* **16,** 3665–3680.

Kodama, K., and G. M. Barnes, 1997: Heavy rain events over the south-facing slopes of Hawaii: Attendant conditions. *Wea. Forecasting,* **12,** 347–367.

Leopold, L. B., 1949: The interaction of trade wind and sea breeze, Hawaii. *J. Meteor.,* **6,** 312–320.

Lyman, R. E., T. A. Schroeder, and G. M. Barnes, 2005: The heavy rain event of 29 October 2000 in Hana, Maui. *Wea. Forecasting,* **20,** 397–414.

Lyons, S. W., 1982: Empirical orthogonal function analysis of Hawaiian rainfall. *J. Appl. Meteor.,* **21,** 1713–1729.

Meehl, G. A., and Coauthors, 2000: An introduction to trends in extreme weather and climate events: Observations, socio-economic impacts, terrestrial ecological impacts, and model projections. *Bull. Amer. Meteor. Soc.,* **81,** 413–416.

Moberg, A., and P. D. Jones, 2005: Trends in indices for extremes in daily temperature and precipitation in central and western Europe, 1901-99. *Int. J. Climatol.,* **25,** 1149–1171.

Oki, D. S., 2004: Trends in streamflow characteristics at long-term gaging stations, Hawaii. USGS Scientific Investigations Rep. 2004-5080, 120 pp.

Pall, P., M. R. Allen, and D. A. Stone, 2007: Testing the Clausius–Clapeyron constraint on changes in extreme precipitation under CO_2 warming. *Climate Dyn.,* **28,** 351–363.

Perica, S., and Coauthors, 2009: *Precipitation-Frequency Atlas of the United States*. NOAA Atlas 14, Vol. 4, version 2.0, National Oceanic and Atmospheric Administration/National Weather Service, 120 pp.

Peterson, T. C., and Coauthors, 2002: Recent changes in climate extremes in the Caribbean region. *J. Geophys. Res.,* **107,** 4061, doi:10.1029/2002JD002251.

Ramage, C. S., and T. A. Schroeder, 1999: Trade wind rainfall atop Mount Waialeale, Kauai. *Mon. Wea. Rev.,* **127,** 2217–2226.

Roy, S. S., and R. C. Balling Jr., 2004: Trends in extreme daily precipitation indices in India. *Int. J. Climatol.,* **24,** 457–466.

Schroeder, T. A., 1977: Meteorological analysis of an Oahu Flood. *Mon. Wea. Rev.,* **105,** 458–468.

Solomon, S., D. Qin, M. Manning, M. Marquis, K. Averyt, M. M. B. Tignor, H. L. Miller Jr., and Z. Chen, Eds., 2007: *Climate Change 2007: The Physical Science Basis*. Cambridge University Press, 996 pp.

Taylor, G. E., 1984: Hawaiian winter rainfall and its relation to the Southern Oscillation. *Mon. Wea. Rev.,* **112,** 1613–1619.

Tebaldi, C., K. Hayhoe, J. M. Arblaster, and G. A. Meehl, 2006: Going to the extremes: An intercomparison of model-simulated historical and future changes in extreme events. *Climatic Change,* **79,** 185–211.

Wilks, D. S., 2006: *Statistical Methods in the Atmospheric Sciences*. 2nd ed. Academic Press, 648 pp.

Zhai, P., A. Sun, F. Ren, X. Liu, B. Gao, and Q. Zhang, 1999: Changes of climate extremes in China. *Climate Change,* **42,** 203–218.